

# Patient-Specific Three-Dimensional Torso Models for Analysing Cardiac Activity

Frederique Vanheusden<sup>1</sup>, João Loures Salinet Jr<sup>2</sup>, William B Nicolson<sup>2</sup>, Gerry P McCann<sup>2,3</sup>,  
G André Ng<sup>2,3</sup>, Fernando S Schlindwein<sup>1,2</sup>

<sup>1</sup>Bioengineering Research Group, University of Leicester, Leicester, United Kingdom

<sup>2</sup>Department of Cardiovascular Sciences, University of Leicester, Leicester, United Kingdom

<sup>3</sup>NIHR Leicester Cardiovascular Biomedical Research Unit, Leicester, United Kingdom

## Abstract

Standard electrocardiogram (ECG) is routinely used for recording cardiac electrical activity but lacks 3D details. Body surface potential mapping techniques have been developed more recently. A major challenge related to this technique is the projection of body signals back to their original sources in the heart. For an accurate projection, one needs to take into account patient-specific electrophysiological data of tissues surrounding the heart. Much information regarding physiological variations, as well as the exact position of organs in the torso, can be obtained from magnetic resonance (MR) images.

Here, a patient-specific methodology for building 3D torso models from transverse MR images is proposed. Torso contour detection is based on edge detection using a canny filter and indicating contour points with a polar coordinate system. Organ detection is performed using an interpolation technique with Active Contour modelling. Results show that accurate torso models can be constructed with short processing time.

## 1. Introduction

Since its inception in 1895, the standard electrogram (ECG) has been established as the main clinical tool to record cardiac electrical activity by placing electrodes on the body surface [1]. Whilst this relatively straightforward technique gives accurate information of heart rate, rhythm and insights into aspects of cardiac (patho)physiology, detailed 3D information is lacking. More recently, body surface potential mapping techniques have been developed to address this [2].

One of the biggest challenges in these techniques is the estimation of cardiac sources from signals obtained at the body surface [3]. This inverse problem needs to take into account many (electro-)physiological aspects, which are tissue- and, in most cases, patient-specific. Attention should be given to provide patient-specific data to build

up the most accurate volume conductor model. In a first step, the position of the organs within the torso should be well-defined to relate body surface signals accurately with the original source.

On the other hand, fast analysis of cardiac activity is desired for optimal patient care. It is therefore important to keep the amount of data manageable and easy to interpret. Generally, however, this type of analysis conflicts with the desire for specificity.

This research attempts to derive the most desirable parameters by providing sufficient details for patient-specific analysis without losing the requirements for rapid processing. The development of 3D torso models is considered in this paper. Figure 1 shows a general overview of the modelling algorithm. Results showed the possibility to reconstruct a complete torso model within 10 minutes with sufficient accuracy. More detailed reconstruction significantly increased processing time. Future research will explore ways to optimise the modelling algorithms and using Finite Element (FE) analysis for reconstructing the sources of cardiac activity responsible for cardiac arrhythmias in various disease states.

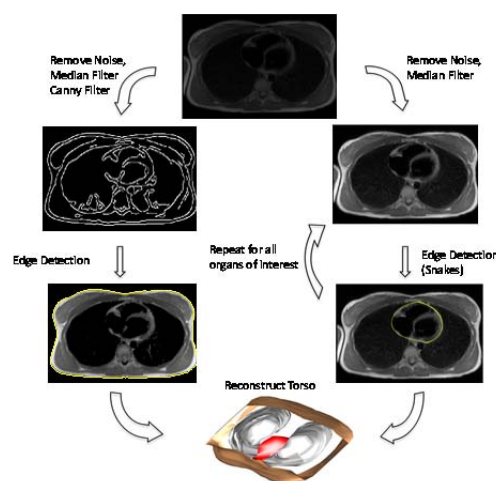


Figure 1. Overview of the torso segmentation algorithm used for reconstruction of the 3D model.

## 1.1. Active contour models

Active Contour Models (snakes) were first described by Kass *et al.* as a means for dynamic image segmentation using local image energy minima [4]. This type of algorithm has been used previously in discretising biomedical images, showing satisfactory results [5].

As described by Kass *et al.* the basic idea for the snake algorithm to segment images lies in the description of energy functions for specific image characteristics: lines, edges and corners or terminations. The total energy of the image is the sum of these functions with a constant for weight adjustment [4]:

$$E_{image} = u_{line}E_{line} + v_{edge}E_{edge} + w_{stop}E_{stop} \quad (1)$$

Here,  $E_{line}$ ,  $E_{edge}$  and  $E_{stop}$  are the energy functions to detect lines, edges and terminations in the image, respectively. The factors  $u_{line}$ ,  $v_{edge}$  and  $w_{stop}$  are the weight constants for the respective energy functions. These constants can be adjusted to make the snake more attracted to one of the individual energy functions. By determining local minima the movement of the snake can be controlled. This can be combined with energy functions of user-defined constraints (e.g. addition of starting points) and the internal energy of the spline function to control the snake's behaviour.

Although there are certain limitations using snakes [6], we considered their use as a first step to obtain patient-specific data.

## 2. Materials and methods

In this section, the algorithms for data processing will be described. Image processing was performed using a desktop with 3.4 GHz Intel i7-2600 core and 16 Gb RAM memory. Images were transferred to MATLAB R2012a software for further image processing.

### 2.1. MR images

Five healthy volunteers were studied on a 1.5T MRI scanner (Avanto, Siemens, Erlangen, Germany) with a 6 channel phased array cardiac coil. Thirty to forty transverse thoracic images were obtained during free breathing with a black blood spin echo sequence (HASTE). Slice thickness was 8 mm with 0 gaps. All subjects provided written informed consent. The study was approved by the local Research Ethics Committee according to the Declaration of Helsinki.

### 2.2. General image processing

First, an intensity threshold filter was therefore applied onto the image. This filter was set such that voxels with

intensity lower than ten per cent of the maximum were removed. A median filter was applied on 3x3 voxel areas to further reduce noise and smoothen up torso boundaries. This filter replaced the intensity of the central element to the median value of its neighbourhood.

### 2.3. Torso edge detection

The next step in torso reconstruction was to detect torso edges. Edge isolation was performed using a canny filter [7]. This filter determines local maxima for the gradient of the intensity function (Gaussian function derivative). Two thresholds are then applied to this function to detect strong and weak edges. Strong edges are always shown on the new image. Weak edges are only included if they are connected to strong edges.

The standard deviation of the Gaussian derivative and the threshold values were optimised for edge isolation. Standard deviation was varied between 0 and 5. The optimum deviation was found to be as low as 1, ensuring that the torso boundary was highlighted. Average optimal threshold values for all images were calculated heuristically from an image training set of 30 images, taking into account the threshold calculated using Otsu's method [8] for converting images to binary images (Figure 2).

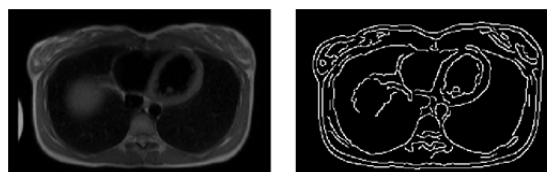


Figure 2. Comparison of amplified image (left) with filtered image (right). The canny filter allows accurate detection of the torso boundary.

To determine the coordinates of the surface, the midpoint of the image was taken as origin. The image was screened for edges using a polar coordinate system, similar to a carousel. The amount of edge points that the algorithm detects can be changed by the user by defining the angle between two points on the coordinate system. For the purpose of this study, the angle was varied between 1° and 9°. Examples for 6° (60 torso points) and 1° (360 points) angles between coordinate points are shown in Figure 3. A difficulty existed in the appearance of the arm and other unwanted regions in certain slices. To avoid detecting these parts as torso edges, the coordinates of prior MRI slices was used for edge detection adjustments.

### 2.4. Organ discretisation

The next step considered the inclusion of organs in the 3D model using Snake algorithms. The original image

processing allowed removing ‘lone voxels’, thereby stopping the snake to ‘jump away’ from the organ contour. Interpolation based on active contour modelling was performed on individual slices. An example of the interpolation output for the heart is shown in Figure 4.

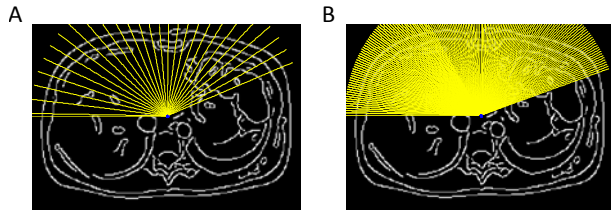


Figure 3. Overview of the polar coordinate (Carousel) algorithm for torso edge detection, shown on the filtered images. The algorithm will identify points at equi-angle steps defined by the user (yellow lines). Figure 3A shows the point detection for  $6^\circ$  angles between points. Figure 3B shows detection for  $1^\circ$  angles.

## 2.5. 3D model and electrode addition

The 3D torso model was reconstructed by combining the extracted edge point for the organs of individual slices. Afterwards, these images were restacked taking into account the thickness of the individual slices.

As a last step, the positions of a standard 12-lead ECG system and a 128-electrode BSPM system were added. The reason for choosing 128 electrodes is based on the system that will be used by the research group for future analysis. The algorithm is however built up such that it can be easily modified to different electrode setups. Adding the electrode positions to the model will facilitate linking electrophysiological output directly to the torso, and could therefore help in further cardiac signal analysis.

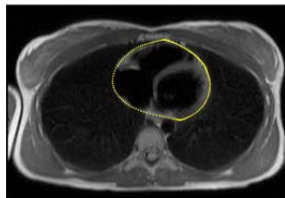


Figure 4. Example of a snake finding the contours of the heart.

## 3. Results and discussion

### 3.1. Torso edge detection

Results were analysed on quality of the model and processing time. For torso edge detection, the amount of points per slide was varied between 40 and 360 points. Figure 5 shows the resulting 3D models based on 60, 120 and 360 points, respectively. As expected, the more points per slice are detected with the algorithm, the more details are shown on the torso model (Figure 5A to C). One has to take into account however, which of these

details are relevant for an accurate reproduction and which are due to small inconsistencies in the images, reducing the smoothness of the model. The amount of nodes for future FE analysis was also considered.

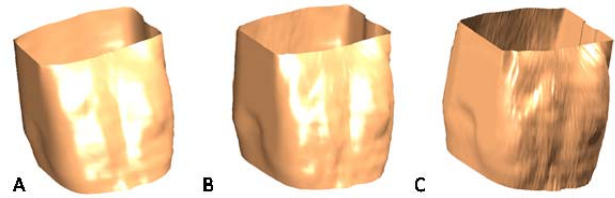


Figure 5. Reconstructed 3D models for one patient. A) for 60 points per slice. B) 120 points. C) 360 points.

A total of 60 edge starting points for a complete torso surface interpolation seems optimal for an accurate reproduction. Using these settings, and considering thirty to forty images per patient, a total of 1800-2400 torso points can be generated, which is considered sufficient to exploit cardiac activity analysis using FE methods. An extra analysis was performed to determine the effect of the amount of torso points detected per MR image on the processing speed and accuracy of the model. The processing speed for different amounts of edge points is shown in Figure 6. The average was taken over all 5 patients.

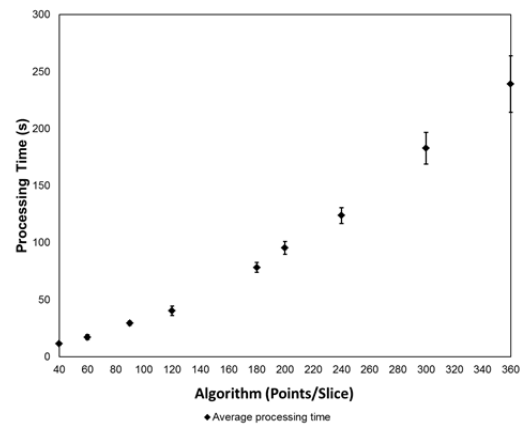


Figure 6. Average processing speed for different torso modelling algorithms taken over 5 patients. Standard deviations are shown with error bars.

It is clear that increasing the amount of detection points per slice has a significant effect on processing speed. The variation in processing time also increases, since the time to process individual slices is larger and there is a variation in number of slices between patients. Generally, these results further justify the idea of not using more than 60 points per slice for 3D modelling.

### 3.2. Organ discretisation

The semi-automatic snake algorithm was started up by

manually specifying landmark points on the MR images. The reasons for this are a lack of sufficient data for developing automatic average organ appearance models and difficulties in optimizing the algorithm for low-quality data. However, after interpolation using the snakes, a sufficiently defined image of both the heart and lungs could be obtained. A complete model with organs is shown in Figure 7. Future research will be conducted to improve organ discretisation.

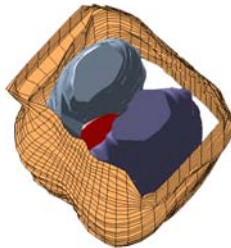


Figure 7. Example of a torso model with organs (heart in red, lung in grey) identified.

Lastly, the addition of Body Surface Potential Measurement (BSPM) system electrodes onto the model is shown (Figure 8). The algorithm calculates the position of the standard 12-lead electrodes first. The position of the BSPM electrodes can then be allocated at equidistant distances from these coordinates. The algorithm is adaptable to any desired BSPM configuration. The addition of the electrodes onto a patient-specific model could help clinicians to apply the system in a more reproducible manner.

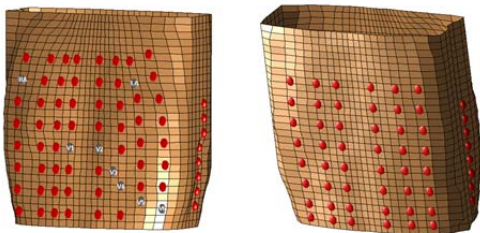


Figure 8. Torso mesh after addition of electrodes. The grey dots suggests positions for the standard 12-lead ECG. The red dots represent position for a 128 electrode BSPM system. Left: Anterior view. Right: Posterior view.

#### 4. Limitations

Although the results show the possibility to develop patient-specific 3D models of the torso and heart, some limitations have to be taken into account. The most important problem is the lack of sufficient data for the development of detailed organ appearance models. By increasing the training set, it will be possible to improve

the snake algorithm. Further research will be directed towards improving organ edge detection.

#### 5. Conclusions

An algorithm for patient-specific 3D torso models including organ modelling is proposed. The paper shows the possibility to develop these models with sufficient accuracy. The algorithms also show flexibility to adapt to the image(s) under investigation. Future research will allow for analysis of cardiac body signals and their projection back to the heart source based on finite elements using these 3D models.

#### Acknowledgements

F. Vanheusden is funded by the National Institute for Health Research (NIHR) Leicester Cardiovascular Biomedical Research Unit. G. McCann is supported by a NIHR Postdoctoral research fellowship. This study is part of the research portfolio supported by the NIHR Leicester Cardiovascular Biomedical Research Unit.

#### References

- [1] Einthoven W. On the shape of human electrocardiograms. *Pflug. Archiv.* 1895;60:101-123 (German).
- [2] Taccardi B. Distribution of heart potentials on the thoracic surface of normal human subjects. *Circ. Res.* 1963;12:341-352.
- [3] Cheng LK, Bodley JM, Pullan AJ. Effects of Experimental and Modeling Errors on Electrocardiographic Inverse Formulations. *IEEE Trans. Biomed. Eng.* 2003;50:23-32.
- [4] Kass M, Witkin A, Terzopoulos D. Snakes: Active Contour Models. *Int. J. Comput. Vision* 1988;1:321-331.
- [5] Nguyen D, Masterson K, Vallée J-P. Comparative Evaluation of Active Contour Model Extensions for Automated Cardiac MR Image Segmentation by Regional Error Assessment. *Magn. Reson. Mater. Phy* 2007;20:69-82.
- [6] Cootes TF, Taylor CJ, Cooper DH, Graham J. Active Shape Models: Their Training and Application. *Comput. Vis. Image Und.* 1995;61:38-59.
- [7] Canny J. A Computational Approach to Edge Detection. *IEEE Trans. Pattern Anal. Mach. Intel.* 1986;8:679-698.
- [8] Otsu N. A Threshold Selection Method from Gray-Level Histograms. *IEEE Trans. Syst. Man. Cyb.* 1979;9:62-66.

Address for correspondence.

Frederique Vanheusden  
 Engineering Department,  
 University of Leicester,  
 University Road, Leicester,  
 LE1 7RH, United Kingdom  
 E-mail: fjv2@le.ac.uk